JCTC Journal of Chemical Theory and Computation

Structural Dynamics of Thrombin-Binding DNA Aptamer d(GGTTGGTGTGGTTGG) Quadruplex DNA Studied by Large-Scale Explicit Solvent Simulations

Roman Reshetnikov*

Department of Boiengineering and Bioinformatics, Lomonosov Moscow State University, GSP-1, Leninskie Gory, Moscow, 119991, Russian Federation

Andrey Golovin

Department of Boiengineering and Bioinformatics, Lomonosov Moscow State University, GSP-1, Leninskie Gory, Moscow, 119991, Russian Federation

Vera Spiridonova

A.N.Belozersky Institute of Physical Chemical Biology, Lomonosov Moscow State University, GSP-1, Leninskie Gory, Moscow, 119991, Russian Federation

Alexei Kopylov

Chemistry Department, Lomonosov Moscow State University, Gsp-1, Leninskie Gory, Moscow, 119991, Russian Federation

Jiří Šponer

Institute of Biophysics, Academy of Sciences of the Czech Republic, Královopolská 135, 61265 Brno, Czech Republic

Received May 13, 2010

Abstract: The thrombin-binding aptamer (15-TBA) is a 15-mer DNA oligonucleotide with sequence d(GGTTGGTGTGGTTGG). 15-TBA folds into a quadruplex DNA (G-DNA) structure with two planar G-quartets connected by three single-stranded loops. The arrangement of the 15-TBA-thrombin complex is unclear, particularly with respect to the precise 15-TBA residues that interact with the thrombin structure. Our present understanding suggests either the 15-TBA single stranded loops containing sequential thymidines (TT) or alternatively a single-stranded loop, containing a guanine flanked by 2 thymidines (TGT), physically associates with thrombin protein. In the present study, the explicit solvent molecular dynamics (MD) simulation method was utilized to further analyze the 15-TBA-thrombin three-dimensional structure. Functional annotation of the loop residues was made with long simulations in the parmbsc0 force field. In total, the elapsed time of simulations carried out in this study exceeds 12 microseconds, substantially surpassing previous G-DNA simulation reports. Our simulations suggest that the TGT-loop function is to stabilize the structure of the aptamer, while the TT-loops participate in direct binding to thrombin. The findings of the present report advance our understanding of the molecular structure of the 15-TBA-thrombin structure further enabling the construction of biosensors for aptamer bases and the development of anticoagulant agents.

10.1021/ct100253m
Published on Web 09/23/2010

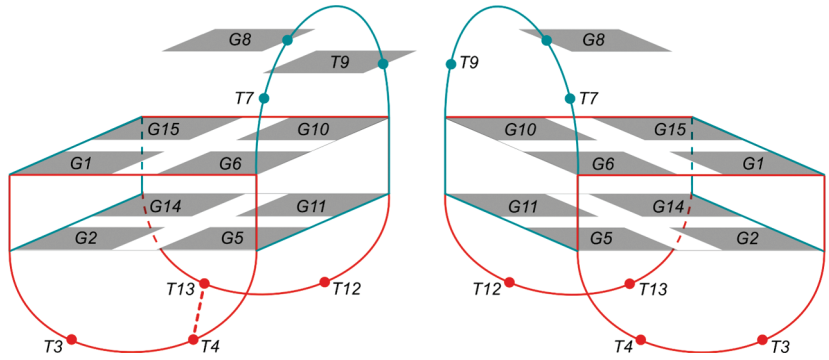

Figure 1. Schematic representation of 15-TBA. Left: NMR-based model. Right: X-ray-based model. Two G-quartets, upper (G1, G6, G10, G15) and lower (G2, G5, G11, G14), form G-quadruplex. The remaining nucleotides form three lateral loops, one TGT and two TT. An approximate 2-fold axis of symmetry relates the two halves of the G-quadruplex, resulting in two symmetric wide grooves (blue) and two symmetric narrow grooves (red). The 15-TBA models differ in chain direction and in loop topology. In the NMR-based model, two nucleic bases from the TGT-loop, G8 and T9, are stacked with the upper G-quartet. Stacking nucleotides from the TGT-loop are shown by gray tetragons. There are T4-T13 pair interactions between the TT-loops. In the X-ray-based model, only the G8 base is stacked with the upper G-quartet with no interactions between the TT-loops.

Introduction

Aptamers are synthetic oligonucleotides that specifically bind with high affinity a wide range targets, from small molecules to whole cells.[1,2] Aptamers have been developed through the use of Systematic Evolution of Ligands by Exponential Enrichment (SELEX).[3] Among the first successful SELEX targets was the serine protease thrombin, which plays a key role in blood coagulation cascade.[4] Thrombin is a globular protein with two positively charged substrate (ligand) binding domains positioned on opposite sides of the protein surface.[5] These substrate binding domains are termed fibrinogen-binding site (exosite I) and heparin-binding site (exosite II) (Supporting Information, Figure S1). The most widely studied thrombin-binding DNA aptamer is the 15-mer oligonucleotide with sequence d(GGTTGGTGTGGTTGG) (15-TBA).[6−10] 15-TBA forms secondary structure consisting of two planar G-quartets, one over another (G-quadruplex or G-stem), connected by three intervening lateral loops. Two of these loops consist of a pair of thymidine bases (TT), while the third loop consists of two thymidines flanking a central guanine base (TGT) (Figure 1).

Despite numerous reports on the structure of 15-TBA, the precise structure and points of interaction with thrombin remain poorly resolved. Both NMR[6−9] and X-ray[10] structures have been reported for 15-TBA. The respective models are mutually inconsistent however, differing both in chain direction and loop geometry. The NMR resolved structure is widely favored over the X-ray structure. Indeed, the NMR structure is in better agreement with the raw X-ray data because of the R-factor and real space correlation coefficient.[11] The NMR-based and X-ray-based 15-TBA models differ with respect to which bases associate directly with thrombin. In the NMR-based model, 15-TBA binds the exosite-I site of thrombin through the TT-loops. Alternatively, the X-ray resolved model suggests that it is the TGT-loop associating directly with exosite-I.[9] Mutational analysis of 15-TBA demonstrates that modification of the TT-loops diminishes thrombin binding.[12,13] However, modification of the TGT-loop sequence of 15-TBA adversely affects thrombin inhibition activity.[14] The stoichiometry of the thrombin-aptamer complex also remains unclear. Bock[4] and Tasset[15] with colleagues have assumed 1:1 stoichiometry of the aptamer-thrombin complex. In contrast, crystallographic data from Padmanabhan et al.[10] suggest that 15-TBA can also interact with exosite-II of a symmetry-related molecule of neighboring thrombin. The crystallographic data is consistent with the isothermal titration calorimetry (ITC) results reported by Pagano et al.,[16] which accordingly demonstrate 2:1 stoichiometry for the thrombin-aptamer complex.

Molecular dynamics simulation (MD) is a valuable tool for investigating G-quadruplex-containing structures.[17−22] Current force fields, such as the parm99[23,24] version of the Cornell et al. force field,[25] can be readily used to provide descriptions of G-stem structures.[17,18] In contrast, diagonal and propeller loops of G-quadruplex structures have previously been difficult targets in molecular modeling approaches.[17−19] In 2007, the parmbsc0 version of the nucleic acids force field was released.[26] The parmbsc0 has since been used to describe correctly a wide range of canonical and noncanonical nucleic acid structures.[26,27] The parmbsc0 version enabled a dramatically improved description of B-DNA structure (which was unstable in longer simulations with earlier versions of the Cornell et al. force field). Parmbsc0 also improves the description of single stranded DNA loop structures (such as those of G-DNA). Albeit, there remain limitations with respect to the capacity of the parmbsc0 force field to yield complete loop descriptions.[19]

Two previously published studies have applied short MD simulations to 15-TBA. Pagano et al.[16] reported that MD simulations of 15-TBA and its derivatives produce stable 5 ns-long trajectories in the parm98 force field. Importantly, the resulting average structure agrees well with the published, NMR-based structure that is the starting model for MD. The lateral loops of 15-TBA are represented well in the parm98 force field though the short simulation time scale precludes definitive conclusions. In a simulation published by Jayapal et al.,[28] predistorted 15-TBA recovers a structure similar to

* To whom correspondence should be addressed. E-mail: r.reshetnikov@gmail.com.

the initial 15-TBA structure during 2 ns of MD in an OPLS-AA force field using entries for nucleic acids added by Golovin and Polyakov.[29] The 2 ns simulations, however, provide only limited insights.

The determination of function for each nucleotide of 15-TBA will resolve many of the aforementioned disparities among published reports. In the present study, we provide functional annotation of 15-TBA residues resulting from the use of long MD simulations. We evaluated the viability of a variety of G-quadruplex-containing structures including G-DNA stems as well as complexes of 15-TBA with thrombin. Herein, we report the use of two force fields to resolve these structures, parm99 and parmbsc0, with simulation times from 600 to 900 ns in individual runs. The combined data from these MD simulations exceeds 12 μs surpassing the duration of any currently published simulations of G-DNA structure.

Data from this study suggest that the NMR-based conformation is the only viable 15-TBA structure, either in its free state or in complex with thrombin. These data further suggest that the X-ray resolved conformation is unstable. MD simulations of loop-free two-quartet G-stem, 15-TBA in a free state, and 15-TBA complexed with thrombin show that the TT-loops substantially influence the twist of the G-stem (as compared to simulation with loop-free stem). Interestingly, subsequent binding of thrombin reduces the structural strain on the stem, clearly suggesting a mutual adaptation of the TT-loops, the stem, and the protein. These data further suggest that the principle function of the TGT-loop is to stabilize the G-stem.

Materials and Methods

Computer Modeling. The X-ray-based structure of 15-TBA was taken from the structure of the complex between thrombin and the aptamer, PDB ID 1hut.[10] The NMR-based structure of 15-TBA was taken from PDB entry 148d, eighth frame.[6] The structure of the four-stranded stem consisting of two G-quartets was obtained from the NMR-based structure by removing loop residues. We have also studied NMR and X-ray models of 15-TBA with modified conformations of the TGT-loop named TG(−T), T(−GT), and TG(+T). Here, signs "−" or "+" denote residues whose position was changed to either disrupt (−) or establish (+) base stacking with the upper G-quartet. These models were obtained from the initial conformations by rotating the G8 and T9 locations around dihedral angles γ, ε, and χ using the Pymol, version 1.1, software program.[30] The energy minimization procedure, with the quasi-Newtonian limited memory Broyden−Fletcher−Goldfarb−Shanno (BFGS) algorithm,[31] was applied for modified conformations to remove strain. For simulations of thrombin-aptamer complexes (PDB ID of NMR-based model 1hao,[9] X-ray-based model 1hut[10]), Asp, Glu, and His residues of thrombin were protonated according to the determination by Ahmed et al.[32] Models of 1:2 complexes of 15-TBA with thrombin were obtained from models of the 1:1 complexes (PDB IDs 1hao, 1hut) by generating the packing interactions within 4 Å from the models in the Pymol, version 1.1, software program. The thrombin molecule interacting with the aptamer of the initial model through its exosite-II was then used as a second protein in the 1:2 complex (Supporting Information, Figure S2).

Molecular Dynamics Simulation. The GROMACS 4.0 software package[33,34] was used for simulation and analysis of MD trajectories using the AMBER-99φ and parmbsc0[26] force fields. The AMBER-99φ force field is an improved version of the parm99[23] force field with reconsidered φ torsion potential, developed and adapted to GROMACS by Sorin and Pande.[35] The parmbsc0[26] force field was ported onto GROMACS by us through a modification of the AMBER-99SB[36] force field entries for nucleic acids. Explicit solvent simulations were performed at $T = 300$ K with a time constant for coupling of 0.1 ps under the control of a velocity rescaling thermostat,[37] isotropic constant-pressure boundary conditions under the control of the Berendsen algorithm of pressure coupling[38] with a time constant of 5 ps and application of the particle mesh Ewald method for electrostatic interactions (PME)[39] with grid spacing of 0.178 nm and interpolation order 6. A triclinic box of TIP4P[40] water molecules was added around the DNA to a depth of 15 Å on each side of the solute. Negative charges were neutralized with the addition of sodium cations and positive charges by chloride ions. Additional NaCl was added to a final concentration of 0.1 M to protein-containing systems. In each of the simulations, there were two temperature coupling groups, the first consisting of DNA with K^+ ion and the second consisting of water with Na^+ and Cl^- ions. Protein atoms, when present, were added to the first group. The time step for integration in all simulations was 3 fs. Coordinates were written to output a trajectory file every 6 ps. Data extraction from the trajectory file for analysis was made with a time step of 150 ps. Stabilization of DNA models, except of the specially stipulated simulations, was made by placing of potassium cation in the geometrical center of the G-quadruplex stem, coordinates of the center were calculated as an arithmetic mean value from O6 atoms positions of the quadruplex stem guanines. We used standard AMBER potassium (radius 0.2658 Å and well depth 0.00137 kJ/mol), sodium (radius 0.1868 Å, well depth 0.01589 kJ/mol) and chloride (radius 0.2470 Å, well depth 0.41840 kJ/mol) parameters. Sodium and chloride ions were added to the systems by replacing water molecules at random positions with minimal distance between ions equal to 6 Å. All simulations were done on a "Chebyshev" supercomputer provided by SRCC of Moscow State University. Information about run times and parallelization of the simulations on the supercomputer is provided in Supporting Information (Figure S3). The simulations parameters are provided in Table 1. Analysis of the trajectories was also performed using the GROMACS 4.0 software package. Hydrogen bonds were treated as existing if their lifetime was greater than 50% of the trajectory length. H-bonds were counted for

Table 1. Simulation Parameters

solute[a]	force field	trajectory length (ns)	quantity of atoms					
			DNA	protein	water	Na^+	K^+	Cl^-
G-stem	parmbsc0	700	260	0	12516	3	1	0
G-stem without ion in the center	parmbsc0	10	260	0	12516	4	0	0
X-ray 15-TBA	parm99	900	488	0	22516	13	1	0
X-ray 15-TBA	parmbsc0	900	488	0	19240	13	1	0
NMR 15-TBA	parm99	900	488	0	22524	13	1	0
NMR 15-TBA	parmbsc0	900	488	0	22532	13	1	0
NMR 15-TBA with Na^+ in the center	parmbsc0	900	488	0	22532	14	0	0
NMR 15-TBA without ion in the center	parmbsc0	900	488	0	22528	14	0	0
modified TGT conformations								
TG(+T) X-ray 15-TBA[b]	parmbsc0	900	488	0	18688	13	1	0
TG(−T) NMR 15-TBA[b]	parmbsc0	900	488	0	18312	13	1	0
TG(−T) NMR^{eq} 15-TBA[b,c]	parmbsc0	900	488	0	18968	13	1	0
T(−GT) NMR^{eq} 15-TBA[b,c]	parmbsc0	900	488	0	20532	13	1	0
complexes with thrombin								
X-ray thrombin-aptamer complex	parmbsc0+parm99SB	600	488	4657[d]	104964	49	1	45
NMR thrombin-aptamer complex	parmbsc0+parm99SB	600	488	4658[d]	105104	48	1	45
1:2 X-ray aptamer-thrombin complex	parmbsc0+parm99SB	600	488	9314	155404	71	1	78
1:2 NMR aptamer-thrombin complex	parmbsc0+parm99SB	600	488	9316	155732	71	1	78

[a] One K^+ ion in the central cavity of the G-stem if not specified otherwise. [b] See the text for explanation of the abbreviation. [c] NMR^{eq} indicates that the starting 15-TBA structure is based on preceding MD simulation of the NMR-based structure. The last 100 ns of the 900 ns simulation were used to create the averaged structure which then was manipulated to arrive at the TG(−T) or T(−GT) arrangement. [d] Thrombin molecules in 1hao and 1hut structures differ from each other in aminoacid sequence.

donor−acceptor distances shorter than 3.5 Å with an acceptor−donor-hydrogen angle cutoff of 30°.

Results

Comparison of the NMR-Based and X-ray-Based Models of Free 15-TBA. The relative stability of the alternative models was determined with 900 ns MD simulation runs in both parm99 and parmbsc0 force fields. In this simulation, the X-ray model was treated as a potentially correct conformation of free 15-TBA. The X-ray resolved model completely lost its G-quartets in both force fields however. In either force field, destruction of the G-quadruplex began with the formation of stacking interactions between T4 and T13 under the G-stem with consequent disruption of the lower G-quartet planarity. In the parm99 force field, the structure maintained characteristics of a G-quadruplex structure until reaching 170 ns of MD trajectory. In the case of the parmbsc0 force field, the G-quadruplex collapsed during the first 10 ns (Supporting Information, Figure S4). In sharp contrast the NMR-based structure remained topologically similar to that of the initial structure in both force fields with the exception of some rearrangement of the T-T interactions below the G-stem. In the parmbsc0 force field, T4-T13 hydrogen bonding interactions switched to T4-T12 and T3-T13 interactions, both under the lower G-quartet of the stem. In the parm99 force field, T4-T13 interactions switched to T4-T12, while T13 remained under the lower G-quartet, T3 remained exposed to solution (Figure 2).

Why is the NMR-Based Structure Stable while the X-ray-Based Structure Is Not? The X-ray resolved model of 15-TBA is presumed incorrect. Therefore, the instability of this model in our simulations is not surprising. However, the collapse of the entire X-ray structure that we observed is of interest. The observed instability in either force field suggests that this 15-TBA arrangement is absolutely unstable at the level of a single molecule, a conclusion that can not be directly derived from the experimental data. Because this collapse did not occur in the case of the NMR-based model, we have concluded not only that the NMR-based model is a better candidate structure, but also that the X-ray model is intrinsically not viable at all. The stability of the NMR structure in our exceptionally long simulations indicates reasonable performance in these force fields. Further, the long simulations used in these studies enable us to better understand the forces and factors that shape the 15-TBA molecule relative to available experimental data.

We have specifically attempted to understand the roles of the stem, the loops and the stem-loop mutual influence. The main structural element of 15-TBA is the G-stem, consisting of two G-quartets. In the NMR resolved model, this stem is shielded from water by G8 and T9 above and by the T4−T13 pair below. In the X-ray resolved structure, the stem is shielded only by G8 above and two thymidines that do not interact with each other below. Taken together, there are four structural features that likely influence the stability of the G-stem: the T4−T13 pair under the G-stem, the G8 and T9 bases above the G-stem and a cation residing between the G-quartets. The NMR-based structure incorporates each of these features. The X-ray-based structure, however, has only the T9 base above the G-stem and a cation situated between the G-quartets. The "minimal" two-quartet stem is itself of interest. While stability of the four-quartet stem has been intensely studied by simulations,[41] the two quartet stem likely possesses a substantially different balance of stabilizing forces. Table 2 summarizes simulations carried out to estimate the relative influence of each of the a-fore-mentioned stabilizing factors.

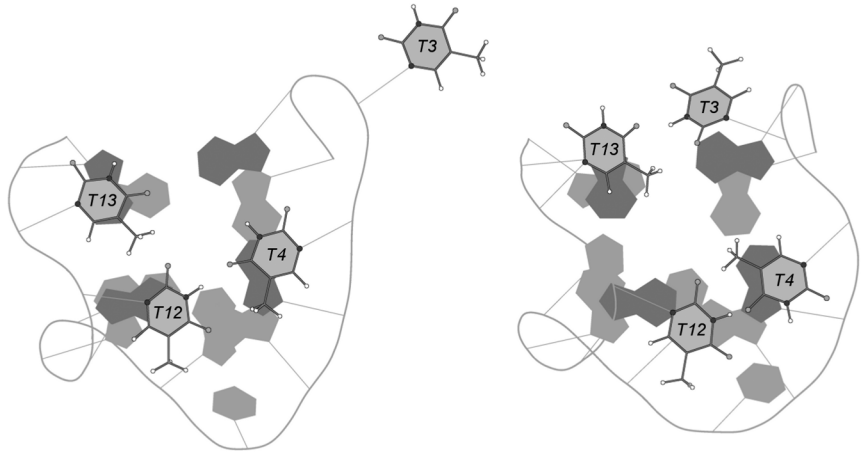

Figure 2. Bottom view of the final MD structure of the NMR-based model of 15-TBA. The structural organization of the TT-loops of the NMR-based model differs depending on the force field used for simulation. In parm99 (left), the T3 thymidine is exposed to solution. After rearrangement, the TT-loops in the parm99 force field acquired, at ~200 ns of MD trajectory, the same geometry as in parmbsc0 force field simulation (right). However, the structure was further changed to the final state at 820 ns of the simulation. In parmbsc0, the four thymidines are stacked with the lower G-quartet (shown in dark gray) forming T3-T13 and T4-T12 pair interactions. This geometry was adopted by loops in the beginning of the simulation and remained unchanged during the entire 900 ns of MD trajectory. Note that the loops are less accurately described by the force fields compared to stems and the results may be force field dependent.[18] Further, the loops may sample multiple conformations so that long simulations may not be statistically converged.

Table 2. Simulations Carried Out to Test the Importance of Specific Factors That May Contribute to the Stability of 15-TBA

system	what was estimated	result
four-stranded G-stem consisting of two G-quartets with K^+ ion between the G-quartets	the influence of the loops on the G-stem stability	the G-stem was stable during all 700 ns of simulation
four-stranded G-stem without stabilizing cation between the G-quartets[a]	importance of stabilizing cation for the G-stem viability	the G-stem was disrupted during the first ns of simulation
NMR 15-TBA model with substitution of stabilizing K^+ ion to Na^+	the influence of different cation parameters on the 15-TBA behavior and geometry	no significant difference between behavior of Na^+- or K^+-stabilized NMR structures
NMR-based 15-TBA model without stabilizing cation between the G-quartets[a]	importance of stabilizing ion for the 15-TBA viability	the model successfully survived, despite fluctuation, until 72 ns of the simulation when bulk Na^+ cation penetrated the center of the G-stem from the bottom through the pore between TT loops (see Figures 2 and 3), fully stabilizing the molecule
NMR-based 15-TBA model with T9 base reoriented away from stacking with the upper G-quartet (TG(-T) NMR)	would the NMR model having only G8 in stacking with the upper G-quartet be viable	the G-quadruplex of the model collapsed with loss of G-quartets, despite of T4-T13 pair in initial structure
X-ray TBA model with T9 base reoriented to establish stacking with the upper G-quartet (TG(+T) X-ray)	would the X-ray model having additional T9 in stacking with the upper G-quartet be viable	the model survived until 789 ns of simulation. Than T4 and T13 formed stacking interactions with each other, which disturbed planarity of the lower G-quartet and resulted in the collapse of the model

[a] That is, there was no ion initially in the channel, while there were obviously ions present in the bulk solvent enabling the stem to capture ions.[42]

Complexes between Thrombin and 15-TBA.

1:1 Complexes. The X-ray-based conformation of 15-TBA simulated above was derived from the structure of the thrombin-aptamer complex (PDB ID 1hut). It is possible that the protein may have influenced the starting structure and simulation behavior of the oligonucleotide in this case. Thus, the dynamic behavior of the NMR-based and X-ray-based models of the thrombin-aptamer complex was tested with 600 ns of MD in the parmbsc0 force field. In the initial structure of the X-ray model of the thrombin-aptamer complex, 15-TBA is anchored on thrombin through the TGT-loop with the TT-loops exposed to solution. The H-bond donor residues of thrombin formed H-bonds not only with the anchored TGT-loop, but also with the T3 nucleotide from the TT-loops. Simulations using this conformation resulted in collapse of the 15-TBA structure with subsequent loss of the G-quartets. The map of hydrogen bonds between the protein and aptamer changed dramatically. There were only 17% of the initially formed H-bonds remaining during simulation (Table 3).

In the initial structure of the NMR-based complex, 15-TBA is anchored to thrombin through the TT-loops with its

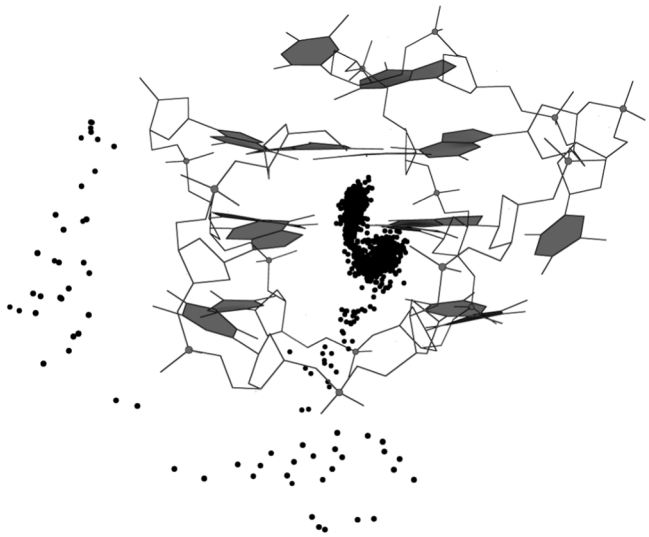

Figure 3. Travel of the Na^+ ion inside the aptamer in the simulation of 15-TBA without stabilizing cation between the G-quartets. This figure represents a period of MD simulation between 60 and 80 ns. The cation (black dots, starting from the left), moving along the phosphodiester backbone of the aptamer, penetrated the interior of 15-TBA between the TT-loops. The Na^+ cation then passed into the G-quadruplex through the lower G-quartet and subsequently remained between the G-quartets for the duration of the simulation. The phosphate atoms of DNA backbone are shown by gray spheres.

top exposed to solution. The resulting MD structure agrees well with the initial structure, with the exception of the orientation of T7 (Figure 4).

The mapping of hydrogen bonds between thrombin and the aptamer reveals much smaller changes of H-bonding pattern than in the simulation using the X-ray-based complex (Table 4). Thirty % of the initially formed H-bonds from the NMR-based structure remained during MD simulation. T3, which is not listed in Table 4, also interacts with thrombin through stacking interactions with Tyr76. Note that the initial structure of the NMR complex is a model.[9] Consequently, loss of some H-bonds is not surprising as they are not based directly on experimentally derived measurement. Importantly, the simulation easily finds alternative H-bonds with no large shift in the overall structure.

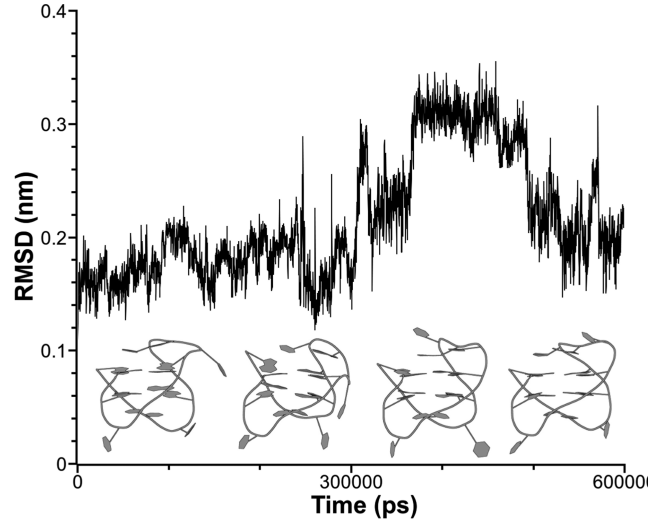

Figure 4. Dynamic behavior of NMR-based 15-TBA in 1:1 complex with thrombin. Snapshots of the aptamer structure are placed at corresponding moments of the trajectory on the rmsd graph. The initial structure of 15-TBA as part of the complex was taken as the reference structure for rmsd calculation, which was made for all atoms of the aptamer. The shift of the rmsd value at 400 ns is related to rearrangement of the TGT-loop; T7 found a new position in stacking with the upper G-quartet.

1:2 Complexes. MD simulation of aptamer-thrombin complexes with 1:2 stoichiometry resulted in only minor changes from the initial models, especially in the case of the NMR-based 15-TBA model. Denoting the thrombin protein from the structure of the aptamer-thrombin complex with 1:1 stoichiometry as thrombin A, and a symmetry-related protein molecule from the neighboring crystal lattice cell as thrombin B, the NMR model of 15-TBA interacts with exosite-I of thrombin A through its TT-loops and with exosite-II of thrombin B through its TGT-loop. These interactions remain unchanged through 600 ns of MD trajectory. T7, which was unbound in the 1:1 complex simulations, interacted with thrombin B. G8 and T9 perfectly shielded the upper G-quartet of the G-stem from charged amino acids and H-bond donors from exosite-II of thrombin B.

Table 3. H-Bonds Map of the X-ray Complex[a]

initial model			dynamical model[b]		
donor	hydrogen	acceptor	donor	hydrogen	acceptor
N3 (T9)	H3 (T9)	OH (Tyr117)	*N3 (T7)*	*H3 (T7)*	*OH (Tyr117)*
N (Ile79)	H (Ile79)	O1P (T9)	*N3 (T3)*	*H3 (T3)*	*OG (Ser72)*
N (Asn78)	H (Asn78)	O1P (T9)	*ND2 (Asn78)*	*HD22 (Asn78)*	*O3′ (T7)*
NH2 (Arg77A)	HH22 (Arg77A)	O4′ (G10)	*ND2 (Asn78)*	*HD22 (Asn78)*	*O2P (G8)*
NH1 (Arg77A)	HH12 (Arg77A)	O4′ (G10)	*N (Asn78)*	*H (Asn78)*	*O2P (G8)*
N (Arg77A)	H (Arg77A)	O3′ (G8)	*N (Tyr76)*	*H (Tyr76)*	*O6 (G8)*
NH2 (Arg75)	HH22 (Arg75)	N7 (G1)	**NH2 (Arg75)**	**HH22 (Arg75)**	**O1P (G8)**
NH2 (Arg75)	**HH22 (Arg75)**	**O1P (G8)**	**NH1 (Arg75)**	**HH12 (Arg75)**	**O1P (G8)**
NH1 (Arg75)	**HH12 (Arg75)**	**O1P (G8)**	*N (Arg75)*	*H (Arg75)*	*O4 (T3)*
NE (Arg75)	HE (Arg75)	N9 (G1)	*OG1 (Thr74)*	*HG1 (Thr74)*	*O3′ (G1)*
NE (Arg75)	HE (Arg75)	N7 (G1)	*N (Thr74)*	*H (Thr74)*	*O4 (T3)*
ND1 (Hys71)	HD1 (Hys71)	O2P (G8)			

[a] H-bonds that were kept during simulation are marked by bold; new H-bonds are marked by italic. [b] Criterion of H-bond existence in MD are described in Materials and Methods section.

Table 4. H-Bond Map of the NMR Complex[a]

initial model			dynamical model[b]		
donor	hydrogen	acceptor	donor	hydrogen	acceptor
N3 (T12)	H3 (T12)	OE2 (Glu77)	*ND2 (Asn 78)*	*HD22*	*O3′ (T13)*
N3 (T12)	H3 (T12)	O (Glu77)	*NH2 (Arg 77A)*	*HH22*	*O1P (G14)*
OG (Ser153)	HG (Ser153)	O4 (T7)	*NH2 (Arg 77A)*	*HH22*	*O4′ (G14)*
OH (Tyr117)	HH (Tyr117)	O1P (T13)	*NH1 (Arg 77A)*	*HH12*	*O (T13)*
N (Asn78)	H (Asn78)	O (T13)	*NH1 (Arg 77A)*	*HH12*	*O5′ (G14)*
NE (Arg77A)	HE (Arg77A)	O1P (G14)	*NH1 (Arg 77A)*	*HH12*	*O4′ (G14)*
N (Tyr76)	**H (Tyr76)**	**O4′ (T4)**	**N (Tyr 76)**	**H**	**O4′ (T4)**
NH2 (Arg75)	**HH22 (Arg75)**	**O (T4)**	**NH2 (Arg 75)**	**HH22**	**O4 (T13)**
NH1 (Arg75)	**HH12 (Arg75)**	**O4 (T13)**	**NH1 (Arg 75)**	**HH12**	**O (T4)**
NE (Arg75)	HE (Arg75)	O (T4)	*NH1 (Arg 75)*	*HH12*	*O4 (T13)*

[a] H-bonds that were kept during simulation are marked by bold; new H-bonds are marked by italic. [b] Criterion of H-bond existence in MD are described in Materials and Methods section.

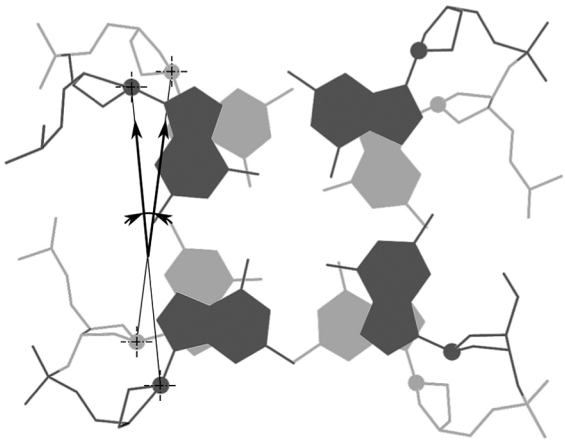

Figure 5. Definition of the twist angle between the two quartets.

In a similar simulation, the X-ray-based model of 15-TBA interacts with exosite-I of thrombin A through its TGT-loop and with exosite-II of thrombin B through its TT-loops. The G-quartet planarity of the aptamer was disrupted early in the MD trajectory. This disturbance did not however result in overall unfolding of the 15-TBA structure. Multiple contacts of the TT-loops with residues of exosite-II of thrombin B anchored this pole of the aptamer structure preventing structural collapse on the observed simulation time scale (Supporting Information, Figure S5).

Structural Dynamics of the G-Stem. Twist Values Indicate Structural Strain. The twist between two adjacent G-tetrads was chosen as an important structural element of the stem. Twist is represented by the angle between two vectors using C1′ atoms of adjacent guanines as the initial and terminal points (Figure 5). We compared the twist angle values and their fluctuations in simulations of free 15-TBA, 15-TBA-protein complexes, and two-quartet stem simulated without the loops (loop-free system). We assumed that the loop-free structure reflects the ideal twist between the two quartets when the stem is not perturbed by other forces.

There are large differences in twist values between the individual structures and in the range of values sampled reflecting the flexibility of the stem (Figure 6). Additionally, there were substantial differences in twist values measured across different grooves. When taking the loop-free stem as a reference, the differences seen in other simulations highlight the influence of the loops on the stem as well as that of protein binding. It is interesting to note that the range of twist values in the deposited 15-TBA NMR-based structure (12 structures, horizontal blue lines in Figure 6) is quite different from values sampled in the simulation of 15-TBA (black time course). This potentially reflects the effect of the simulation force field, which could shift the optimal twist value relative to experimental structures, as is known to be the case for B-DNA simulations. It is important to note that even if the force field is systematically shifting the absolute twist values the simulations would still properly reflect the relative twist values of different structures. However, the twist range in the NMR-based structure could also be affected by the NMR structure refinement protocol, which consists of a simulated annealing run from 1000 to 75 K in 1000 cycles, followed by energy minimization in the X-PLOR 3.1 system. Note also that the NMR-based structure has substantial deformation (nonplanarity) of the quartets which may indicate some inherent conflicts in the NMR-based data (Figure 7 left), while the MD simulation yields regular quartets.

The 15-TBA loops influence the twist value by substantially restricting the structure and flexibility of the stem. As a result, there is a dramatic reduction in the twist value as well as a reduction in its variability (cf. black and gray lines in Figure 6). Indeed, there is nearly no overlap in twist values sampled in simulations of the loop-free stem and complete 15-TBA. Considering that a 100 ns simulation can, assuming Arrhenius kinetics, sample events differing by as much as 7−8 kcal/mol from the free energy minimum, the influence of the loops is significant. Importantly, complex formation of 15-TBA with thrombin mitigates the influence of the loops on the twist value.

Thrombin's influence on the twist angles corresponding to the narrow grooves of 15-TBA (Figure 6A and C, black and brown lines) is slight. Deviations of the twist angle, both in free 15-TBA and 15-TBA complexed with thrombin, is similar when compared to the loop-free G-stem. Thrombin, however, significantly influences the twist angles corresponding to the wide grooves of 15-TBA (Figure 6, B and D). 15-TBA, complexed with thrombin, has a twist angle that is much closer to that of the loop-free G-stem than to that of the free 15-TBA. In the 15-TBA-thrombin complex, thrombin compensates for the influence of the loops on the stem structure at the wide groove, while there is no similar

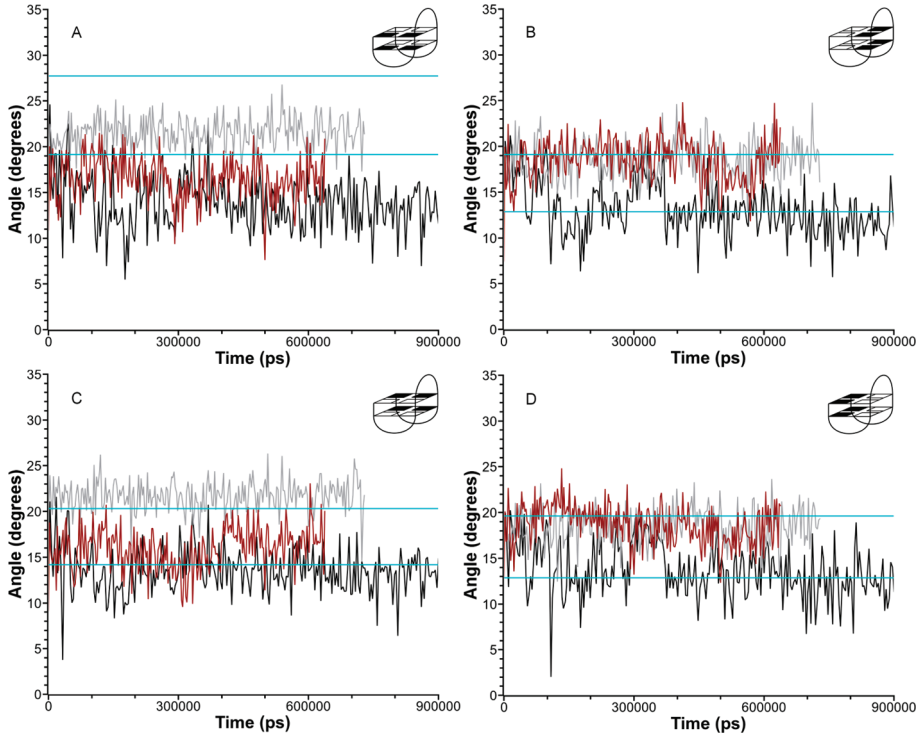

Figure 6. Timed development of the twist angle between the quartets. Twist angle was monitored in different simulations for different grooves, as indicated by the inset structures. Data were smoothed with spline interpolation. Gray: The twist between the two quartets of the four-stranded G-stem without the loops. Black: NMR-based model of 15-TBA in free state. Brown: NMR model in 1:1 complex with thrombin. The two horizontal blue lines demarcate the range of twist values seen in the 12 structures representing the NMR-based model of 15-TBA in PDB entry 148d.

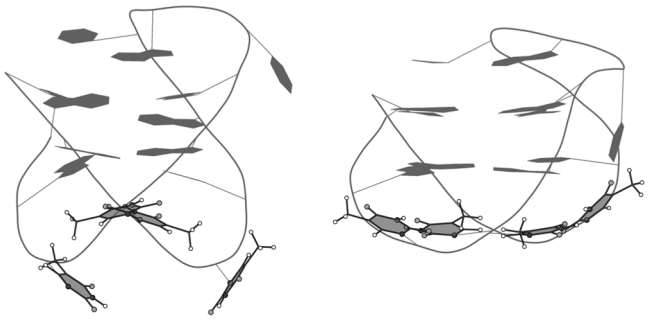

Figure 7. NMR model of 15-TBA before and after MD in parmpsc0 force field. Left: Structure of NMR-based model of 15-TBA from PDB entry 148d. Right: Final MD structure of NMR-based model of 15-TBA. Thymidines from the TT-loops are outlined.

compensation in the narrow groove. The only structural elements of 15-TBA that could influence the geometry of the stem at the narrow groove are the TT-loops which display the greatest rearrangement among the structural elements of 15-TBA during simulations (Figure 7). It seems that the origin of the strains that led to collapse of the X-ray-based 15-TBA structure, as well as the modified TG(-T) NMR-based structure, is the initial geometry of the TT-loops. Two modified 15-TBA models were simulated to test this possibility: 1) the resulting MD NMR-based structure with T9 subsequently reoriented away from stacking with the upper G-quartet (TG(-T) NMR^{eq}) and 2) the resulting MD NMR-based structure with T9 and G8 bases reoriented away from stacking with the upper G-quartet (T(-GT) NMR^{eq}). In the case of both starting structures, the TT-loops are in a conformation that is equilibrated (by the preceding simulations) for minimal negative influence on the G-stem. Both structures successfully survived simulation until the reoriented bases returned to form stacking interactions with the upper G-quartet.

Discussion

The thrombin-binding aptamer (15-TBA) is an intriguing example of a G-DNA containing structure. In addition to its intrinsic affinity for thrombin and potential medicinal value, 15-TBA also represents an important system to study the basic physical chemistry of G-DNA folding and the stabilizing balance of forces. 15-TBA contains the minimum number of G-quartets (just two), raising an interesting question with respect to how is the 15-TBA structure is stabilized? The stability of G-DNA originates primarily from cation-stabilized G-quartet stems. However, the ions within the stem exchange with the bulk solvent. Since the molecule must be regularly exposed to periods when no ion is left in its single ion-binding cavity in the stem, formation of a stable stem with only two quartets is somewhat surprising.

15-TBA contains three short single-stranded loops that maintain proximity between the G-stretches and are essential for thrombin binding. Besides their obvious entropic role (i.e, the difference between forming the stem from either a single strand or from four separate strands), these loops also may exert a direct influence on the stem that may be either stabilizing or destabilizing. Destabilizing effects can arise when the length of the loop is in conflict with the optimal

stem structure while stabilizing effects could be caused by molecular interactions such as base stacking.

Complicating our understanding of 15-TBA structure, conflicting reports based upon X-ray data for the thrombin-aptamer complex and NMR data for free aptamer have been reported. In these disparate reports, there resides a discrepancy in chain orientation. There is also uncertainty with respect to the exact coordination of potassium ions. Marathias and Bolton[8] suggested that two potassium ions bind 15-TBA, while several studies indicate that a single potassium ion binds 15-TBA.[43−45] The putative 2:1 binding stoichiometry may represent an additional stabilizing influence for the two-quartet stem during ion exchange with bulk. The MD simulation technique is a well established tool for the study of monovalent ion binding to nucleic acids, including G-DNA. However, there are inherent limitations in the use of MD for this purpose.[18,19] For example, simple pair-additive force field cannot model polarization of electron clouds, which adversely affects our ability to describe the coordination of ions. Because of this limitation, we elected not to study the detailed difference between the influences of Na^+ and K^+ ions on the 15-TBA structure or analyze exact ion binding patterns, that is, the 2:1 versus 1:1 binding. Nevertheless, we did not observe any population of 2:1 binding in our simulations.

In principle, a desirable, precise evaluation of the described interactions could be achieved using combined quantum/molecular mechanics methods.[46,47] These methods however, are limited in the duration of simulation (dozens of ps) due to substantial computational demand. Though accurate, standard gas phase QM computations on small models are not likely to provide a correct description of the balance of interactions in G-DNA stems. Despite its limitations, MD simulation is capable of substantially contributing to our understanding of the basic role of charge in the 15-TBA quadruplex channel. In the present study, we focused on the comparative study of 15-TBA with published chain orientations, 15-TBA loop-free analogue (two-quartet stem with no loops), and 15-TBA in complex with thrombin using very long MD simulations reaching 12 microsecond of simulation time in total. Our study has two basic parts. We initially investigated the basic properties of free 15-TBA models. We then studied 15-TBA-thrombin complexes using essentially all structural data available in the literature.

The free NMR-based model of 15-TBA is viable in MD simulations, while the X-ray-based model is not. The reason for this difference relates to intramolecular interactions that can either stabilize or disrupt the G-quarduplex structure. Stabilizing interactions refer to the functions of the TGT-loop and a cation that resides within the G-stem. However, the relative importance of these contributions remains uncertain. The NMR-based model of free 15-TBA was viable even when simulated initially without a stabilizing cation. Moreover, the NMR-based model was capable of spontaneously capturing a cation from the bulk to achieve full stabilization. In contrast, the two quartet loop-free stem simulated initially without a bound ion collapsed immediately. However, the two-quartet, loop-free stem was stable if the ion was initially placed into its cavity. Taken together, these simulations reveal the following stability order of the structures used in simulations: 15-TBA NMR-based structure > two quartet stem >15-TBA X-ray-based structure. These data clearly show that the overall effect of the three loops is direct energy stabilization of the 15-TBA NMR-based structure.

When we tried to specifically weaken the structure by initially shifting T9 from the TGT loop to disrupt its stacking with the stem, the molecule was destabilized even in the presence of an internal cation. This observation indicates (albeit does not prove) a potentially important stabilizing role for T9. Obviously, the artificial intervention into the starting structure could introduce undesired destabilization (high-energy deformation) because of strained topology of the TGT loop. The simulation might be subsequently unable to repair such a destabilizing interaction. The dynamics of destabilization indicate that the cause of structural collapse is primarily associated with the conformation of the TT-loops. Once the T9 is unstacked, the TGT loop is unable to counterbalance the strain associated with the TT-loops. However, the electronic part of coordination interactions between the ion and solute could not be included via the force field model. Consequently, the description of the ion's stabilizing role may be imprecise.

Our simulations indicate that there should be at least two nucleotides (G8 and T9) stacked with the upper G-quartet for the molecule's viability. The only remaining residue from the TGT-loop that, according to MD, does not take part in any intramolecular interactions is T7. It seems that this residue merely functions to extend the length of the loop. Indeed, Smirnov and Shafer previously reported that three nucleotides is the optimal length for the central loop.[48] This finding also correlates well with example 11 in the U.S. patent of Griffin et al.,[49] in which modified forms of 15-TBA containing an abasic nucleotide at each position were synthesized. The only mutant with increased thrombin clotting time relative to the unmodified form was the nonbasic T7 substitution (161 s versus 136 s). Each of the remaining mutants demonstrated decreased thrombin clotting time about 30−50 s.

We have several lines of evidence to support the destabilizing influence of the TT-loops on the 15-TBA structure highlighted by the significant effect of the loops on the twist value of the stem (see below and Figure 6). The loops may be too short and cause strain within 15-TBA. Interestingly, in simulations of the 15-TBA NMR-based model, geometries of the TT-loops are substantially remodeled (Figure 7), indicating that their starting structures are suboptimal and relax during simulation. There are two potential explanations to account for the observed remodeling that we cannot readily discern. First, the starting NMR-based geometry is not perfect and the simulation is remodeling to arrive at the correct structure. Second, the geometry of G-DNA loops can also be influenced by force field approximations, as demonstrated in the literature.[19] This would mean that the simulation again increases the stability of the molecule relative to the starting structure. This improvement, however, would be obtained within the approximation of the force field. Interestingly, when we repeated simulation with T9 unstacking using the

15-TBA starting structure equilibrated by our 900 ns simulation (i.e., having relaxed TT loops), the molecule did not collapse as a result of being weakened by shifting of either T9, or both T9 and G8 from their stacking positions. This 15-TBA starting structure survived until the displaced 15-TBA bases returned to their initial stacking positions.

The TT-loops also serve a critical function in the 15-TBA complex with thrombin. The X-ray-based conformation, if correct, would interact with the protein through its TGT-loop. Despite multiple contacts of the top region of the aptamer with exosite-1 that could stabilize the structure of the oligonucleotide (Table 3), the destabilizing influence of the TT-loops was of greater magnitude. In contrast, in the NMR-based model, the TT-loops are in contact with thrombin, rendering the aptamer stem structure less strained (as indicated by the twist values) than the free structure (Figure 6A−D). This observation not only favors the NMR-based model of the complex but also corresponds with data showing that thrombin can serve as a molecular chaperone for 15-TBA in the absence of stabilizing ions.[50]

MD simulations of aptamer-thrombin complexes with 1:2 stoichiometry demonstrate that these structures are stable and may exist. The 1:2 complex based on the X-ray model of 15-TBA confirmed the importance of the TT-loops for thrombin binding. Multiple contacts of the TT-loops with thrombin exosite II anchored the structure of the aptamer, preventing disintegration during the 600 ns of MD trajectory. Tsiang et al. showed that substitution of the thrombin exosite II residues does not affect inhibition of thrombin activity by the aptamer[51] suggesting that 15-TBA either does not bind exosite II of thrombin or binding of 15-TBA to exosite II is not inhibitory. We are examining the later suggestion in ongoing studies.

The stem in the NMR-based 15-TBA structure is evidently strained (deformed) by the presence of TT-loops as is evidenced by the substantial change of the stem twist angle relative to simulation involving a fully relaxed stem without loops. However, the effect of the loops can be complex, as noted above. Data from these simulations are consistent with the suggestion that the TGT-loop stabilizes the stem while the TT-loops induce strain in the stem structure. In agreement with the study of Baldrich and O'Sullivan,[50] binding of thrombin apparently reduces the structural strain exerted by the TT-loops on the stem. Notably, each of these considerations is based indirectly on the analysis of structural dynamics. We did not attempt any free energy calculations as we are unaware of a straightforward procedure to perform the necessary calculations using contemporary simulation methods in a reliable manner.

The present study is based on simulations that are 1−2 orders of magnitude longer than those in the preceding G-DNA simulation studies. Such long simulations give us considerably more confidence in the validity of the results. We have seen several changes after extending the individual simulations beyond 50 ns, so this extension is useful and in any case brings a substantial improvement in the reliability of the simulations, at least as far as the sampling is concerned. Still, we think it would not be appropriate to make any definitive conclusions about convergence of the results, since even 0.1−1.0 μs simulations are short compared to real conformational changes. Further, for the specific system studied here we do not have the highest-resolution X-ray structures available that would be necessary to rigorously benchmark the simulation data. For the present system, actually, there has been a literature controversy about correctness of some of the experimental structures (our long simulations speak clearly in favor of the NMR structure).

In summary, our simulations suggest the following conclusions. The loops have a stabilizing influence on the 15-TBA molecule. However, the TT-loops (although they help to keep the GG-stretches together) have a destabilizing influence on the stem structure. The TGT-loop, in contrast, appears to be in all aspects stabilizing. However, the TT-loops mediate thrombin binding, an interaction that in addition appears to reduce the conflict between the optimal structure of the stem and the short TT-loops. The simulations described herein strongly support the NMR-based model of 15-TBA. The results provided by this study can aid in the construction of biosensors. A potential design of such a biosensor based upon the results of this study would involve the immobilization of the aptamer through its TGT loop. The exposed TT-loops would then project into solution to bind thrombin.

Acknowledgment. Computer resources were provided by the Research Computing Center of Moscow State University. The supercomputer, "Chebyshev", was used for all modeling studies. J.S. was supported by the Grant Agency of the Academy of Sciences of the Czech Republic grant IAA400040802, Grant Agency of the Czech Republic grant 203/09/1476, Ministry of Education of the Czech Republic grant LC06030 and Academy of Sciences of the Czech Republic, Grants AV0Z50040507 and AV0Z50040702. R.R. is grateful to Arthur Zalevsky for his help in the preparation of simulations. This research was also supported by Russian Foundation for Basic Research Grants 08-04-01244-a and 08-04-01540-a and Ministry of Education and Science of the Russian Federation Grant 02.512.11.2242.

Supporting Information Available: Representation of thrombin functional sites, illustration of the creation of the 1:2 complex model, "Chebyshev" supercomputer performance characteristics, collapse of the X-ray model in parmbsc0 force field with rmsd plot, the X-ray-based model of 1:2 complex after MD simulation in barmbsc0 force field and a plot of the radius of gyration of G-quadruplex structures in several simulations. This information is available free of charge via the Internet at http://pubs.acs.org/.

References

(1) Nimjee, S. M.; Rusconi, C. P.; Sullenger, B. A. Aptamers: An emerging class of therapeutics. *Annu. Rev. Med.* **2005**, *56*, 555–583.

(2) Shamah, S. M.; Healy, J. M.; Cload, S. T. Complex target SELEX. *Acc. Chem. Res.* **2008**, *41*, 130–138.

(3) Tuerk, C.; Gold, L. Systematic evolution of ligands by exponential enrichment: RNA ligands to bacteriophage T4 DNA polymerase. *Science* **1990**, *249*, 505–510.

(4) Bock, L. C.; Griffin, L. C.; Latham, J. A.; Vermaas, E. H.; Toole, J. J. Selection of single-stranded DNA molecules that

bind and inhibit human thrombin. *Nature.* **1992**, *355*, 564–566.

(5) Di Cera, E. Thrombin. *Mol. Aspects Med.* **2008**, *29*, 203–254.

(6) Schultze, P.; Macaya, R. F.; Feigon, J. Three-dimensional solution structure of the thrombin-binding DNA aptamer d(GGTTGGTGTGGTTGG). *J. Mol. Biol.* **1994**, *235*, 1532–1547.

(7) Mao, X.; Marky, L. A.; Gmeiner, W. H. NMR structure of the thrombin-binding DNA aptamer stabilized by Sr^{2+}. *J. Biomol. Struct. Dyn.* **2004**, *22*, 25–33.

(8) Marathias, V. M.; Bolton, P. H. Structures of the potassium-saturated, 2:1, and intermediate, 1:1, forms of a quadruplex DNA. *Nucleic Acids Res.* **2000**, *28*, 1969–1977.

(9) Padmanabhan, K.; Tulinsky, A. An ambiguous structure of a DNA 15-mer thrombin complex. *Acta Crystallogr. D* **1996**, *52*, 272–282.

(10) Padmanabhan, K.; Padmanabhan, K. P.; Ferrara, J. D.; Sadler, J. E.; Tulinsky, A. The structure of alpha-thrombin inhibited by a 15-mer single-stranded DNA aptamer. *J. Biol. Chem.* **1993**, *268*, 17651–17654.

(11) Kelly, J. A.; Feigon, J.; Yeates, T. O. Reconciliation of the X-ray and NMR structures of the thrombin-binding aptamer d(GGTTGGTGTGGTTGG). *J. Mol. Biol.* **1996**, *256*, 417–422.

(12) Heckel, A.; Mayer, G. Light regulation of aptamer activity: An anti-thrombin aptamer with caged thymidine nucleobases. *J. Am. Chem. Soc.* **2005**, *127*, 822–823.

(13) Mendelboum Raviv, S.; Horváth, A.; Aradi, J.; Bagoly, Z.; Fazakas, F.; Batta, Z.; Muszbek, L.; Hársfalvi, J. 4-Thiodeoxyuridylate-modified thrombin aptamer and its inhibitory effect on fibrin clot formation, platelet aggregation and thrombus growth on subendothelial matrix. *J. Thromb. Haemost.* **2008**, *6*, 1764–1771.

(14) Ikebukuro, K.; Okumura, Y.; Sumikura, K.; Karube, I. A novel method of screening thrombin-inhibiting DNA aptamers using an evolution-mimicking algorithm. *Nucleic Acids Res.* **2005**, *33*, e108−e108.

(15) Tasset, D. M.; Kubik, M. F.; Steiner, W. Oligonucleotide inhibitors of human thrombin that bind distinct epitopes. *J. Mol. Biol.* **1997**, *272*, 688–698.

(16) Pagano, B.; Martino, L.; Randazzo, A.; Giancola, C. Stability and binding properties of a modified thrombin binding aptamer. *Biophys. J.* **2008**, *94*, 562–569.

(17) Fadrná, E.; Špačková, N.; Štefl, R.; Koča, J.; Cheatham, T. E.; Šponer, J. Molecular dynamics simulations of guanine quadruplex loops: advances and force field limitations. *Biophys. J.* **2004**, *87*, 227–242.

(18) Šponer, J.; Špačková, N. Molecular dynamics simulations and their application to four-stranded DNA. *Methods* **2007**, *43*, 278–290.

(19) Fadrná, E.; Špačková, N.; Sarzyñska, J.; Koča, J.; Orozco, M.; Cheatham, T. E.; Kulinski, T.; Šponer, J. Single stranded loops of quadruplex DNA as key benchmark for testing nucleic acids force fields. *J. Chem. Theory Comput.* **2009**, *5*, 2514–2530.

(20) Haider, S.; Parkinson, G. N.; Neidle, S. Molecular dynamics and principal components analysis of human telomeric quadruplex multimers. *Biophys. J.* **2008**, *95*, 296–311.

(21) Hazel, P.; Parkinson, G. N.; Neidle, S. Predictive modelling of topology and loop variations in dimeric DNA quadruplex structures. *Nucleic Acids Res.* **2006**, *34*, 2117–2127.

(22) Cavallari, M.; Calzolari, A.; Garbesi, A.; Di Felice, R. Stability and migration of metal ions in G4-wires by molecular dynamics simulations. *J. Phys. Chem. B.* **2006**, *110*, 26337–26348.

(23) Cheatham, T. E.; Cieplak, P.; Kollman, P. A. A modified version of the Cornell et al. force field with improved sugar pucker phases and helical repeat. *J. Biomol. Struct. Dyn.* **1999**, *16*, 845–862.

(24) Wang, J.; Cieplak, P.; Kollman, P. How well does a restrained electrostatic potential (RESP) model perform in calculating conformational energies of organic and biological molecules. *J. Comput. Chem.* **2000**, *21*, 1049–1074.

(25) Cornell, W. D.; Cieplak, P.; Bayly, C. I.; Gould, I. R.; Merz, K. M.; Ferguson, D. M.; Spellmeyer, D. C.; Fox, T.; Caldwell, J. W.; Kollman, P. A. A second generation force field for the simulation of proteins, nucleic acids, and organic molecules. *J. Am. Chem. Soc.* **1996**, *118*, 2309.

(26) Pérez, A.; Marchán, I.; Svozil, D.; Sponer, J.; Cheatham, T. E.; Laughton, C. A.; Orozco, M. Refinement of the AMBER force field for nucleic acids: improving the description of α/γ conformers. *Biophys. J.* **2007**, *92*, 3817–3829.

(27) Pérez, A.; Luque, F. J.; Orozco, M. Dynamics of B-DNA on the microsecond time scale. *J. Am. Chem. Soc.* **2007**, *129*, 14739–14745.

(28) Jayapal, P.; Mayer, G.; Heckel, A.; Wennmohs, F. Structure-activity relationships of a caged thrombin binding DNA aptamer: Insight gained from molecular dynamics simulation studies. *J. Struct. Biol.* **2009**, *166*, 241–250.

(29) Golovin, A.; Polyakov, N. OPLS-AA/L force field entries for nucleic acids. http://rnp-group.genebee.msu.su/3d/ff.htm (accessed Feb 22, 2005).

(30) *The PyMOL Molecular Graphics System*, version 1.1, Schrödinger LLC. http://www.schrodinger.com/ (accessed Sep 20, 2010).

(31) Byrd, R. H.; Lu, P.; Nocedal, J.; Zhu, C. A limited memory algorithm for bound constrained optimization. *SIAM J. Sci. Comput.* **1995**, *16*, 1190.

(32) Ahmed, H. U.; Blakeley, M. P.; Cianci, M.; Cruickshank, D. W. J.; Hubbard, J. A.; Helliwell, J. R. The determination of protonation states in proteins. *Acta Crystallogr. D* **2007**, *63*, 906–922.

(33) van der Spoel, D.; Lindahl, E.; Hess, B.; Groenhof, G.; Mark, A. E.; Berendsen, H. J. C. GROMACS: Fast, flexible, and free. *J. Comput. Chem.* **2005**, *26*, 1701–1718.

(34) Hess, B.; Kutzner, C.; van der Spoel, D.; Lindahl, E. GROMACS 4: Algorithms for highly efficient, load-balanced, and scalable molecular simulation. *J. Comput. Chem.* **2008**, *4*, 435–447.

(35) Sorin, E. J.; Pande, V. S. Exploring the helix-coil transition via all-atom equilibrium ensemble simulations. *Biophys. J.* **2005**, *88*, 2472–2493.

(36) Hornak, V.; Abel, R.; Okur, A.; Strockbine, B.; Roitberg, A.; Simmerling, C. Comparison of multiple Amber force fields and development of improved protein backbone parameters. *Proteins* **2006**, *65*, 712–725.

(37) Bussi, G.; Donadio, D.; Parrinello, M. Canonical sampling through velocity rescaling. *J. Chem. Phys.* **2007**, *126*, 014101−014107.

(38) Berendsen, H. J. C.; Postma, J. P. M.; van Gunsteren, W. F.; DiNola, A.; Haak, J. R. Molecular dynamics with coupling to an external bath. *J. Chem. Phys.* **1984**, *81*, 3684–3690.

(39) Darden, T.; York, D.; Pedersen, L. Particle mesh Ewald: An *N* log(*N*) method for Ewald sums in large systems. *J. Chem. Phys.* **1993**, *98*, 10089–10092.

(40) Jorgensen, W. L.; Chandrasekhar, J.; Madura, J. D.; Impey, R. W.; Klein, M. L. Comparison of simple potential functions for simulating liquid water. *J. Chem. Phys.* **1983**, *79*, 926–935.

(41) Štefl, R.; Cheatham, T. E.; Špačková, N.; Fadrná, E.; Berger, I.; Koča, J.; Šponer, J. Formation pathways of a guanine-quadruplex DNA revealed by molecular dynamics and thermodynamic analysis of the substates. *Biophys. J.* **2003**, *85*, 1787–1804.

(42) Špačková, N.; Berger, I.; Šponer, J. Structural dynamics and cation interactions of DNA quadruplex molecules containing mixed guanine/cytosine quartets revealed by large-scale MD simulations. *J. Am. Chem. Soc.* **2001**, *123*, 3295–3307.

(43) Hud, N. V.; Smith, F. W.; Anet, F. A.; Feigon, J. The selectivity for K^+ versus Na^+ in DNA quadruplexes is dominated by relative free energies of hydration: a thermodynamic analysis by 1H NMR. *Biochemistry.* **1996**, *35*, 15383–15390.

(44) Vairamani, M.; Gross, M. L. G-quadruplex formation of thrombin-binding aptamer detected by electrospray ionization mass spectrometry. *J. Am. Chem. Soc.* **2003**, *125*, 42–43.

(45) Majhi, P. R.; Qi, J.; Tang, C.; Shafer, R. H. Heat capacity changes associated with guanine quadruplex formation: an isothermal titration calorimetry study. *Biopolymers.* **2008**, *89*, 302–309.

(46) Car, R.; Parrinello, M. Unified approach for molecular dynamics and density-functional theory. *Phys. Rev. Lett.* **1985**, *55*, 2471–2474.

(47) Eichinger, M.; Tavan, P.; Hutter, J.; Parrinello, M. A hybrid method for solutes in complex solvents: Density functional theory combined with empirical force fields. *J. Chem. Phys.* **1999**, *110*, 10452–10467.

(48) Smirnov, I.; Shafer, R. H. Effect of loop sequence and size on DNA aptamer stability. *Biochemistry* **2000**, *39*, 1462–1468.

(49) Griffin, L. C.; Albrecht, G.; Latham, J. A.; Leung, L.; Vermaas, E.; Toole, J. J. Aptamers specific for biomolecules and methods of making. U.S. Patent 5756291, May 26, 1998.

(50) Baldrich, E.; O'Sullivan, C. K. Ability of thrombin to act as molecular chaperone, inducing formation of quadruplex structure of thrombin-binding aptamer. *Anal. Biochem.* **2005**, *341*, 194–197.

(51) Tsiang, M.; Jain, A. K.; Dunn, K. E.; Rojas, M. E.; Leung, L. L. K.; Gibbs, C. S. Functional mapping of the surface residues of human thrombin. *J. Biol. Chem.* **1995**, *270*, 16854–16863.

CT100253M